A PRACTICAL CHARACTERISATION FOR VIBRO-ACOUSTIC SOURCES IN BUILDINGS

B. M. Gibbs, N. Qi and A. T. Moorhouse*

Acoustics Research Unit, School of Architecture, University of Liverpool, L69 3BX

***** Acoustics Research Centre, University of Salford, Salford M5 4WT, UK.

Abstract

This paper considers a practical structure-borne sound source characterisation for mechanical installations in buildings. Such machines nearly always are installed in contact with heavyweight homogeneous structural floors and walls, or floating floor systems, or stiffened cavity constructions. Manufacturers require a laboratory-based measurement procedure, which will yield single values of source strength in a form transferable to a prediction of the sound power generated in the installed condition, and thence the sound pressure in rooms removed from the source. A novel reception plate method is proposed which yields the source activity in the form of the sum of the squared free velocities, over the contact points. In addition, the source mobility is obtained separately as the average of the magnitude of the effective mobility, over the contact points. Both quantities can be used to estimate the installed power for the range of receiver mobilities likely to be encountered in buildings. It is demonstrated that the installed power can be estimated by reference to a high source mobility condition, a low source mobility condition, or to a matched mobility condition.

1. INTRODUCTION

The topic of structure-borne sound sources is receiving increased consideration in response to calls for practical source characterisations, which will yield data and methods useful for vibro-acoustic transmission prediction and control, and for low noise product design. These calls come from manufacturers of machines and machine components, which are sources of vibration and noise in assembled products, from designers requiring prediction methods in low-noise product development and from authors of standards on noise from installed products. There have been reviews of this topic by Bodén [1], Olhrich [2] and ten Wolde and Gadefelt [3], and comprehensive introductions in papers by Verheij [4], Petersson and Gibbs [5] and Moorhouse [6].

There are two main challenges in seeking a structure-borne source characterisation, when compared with the case of air-borne sources [1]. First, a source characterisation, based on structure-borne transmission, requires consideration of the structural dynamics of both the source and receiving systems and the latter seldom can be known in detail. Secondly, the transmission process is complicated and a full description requires a large data set. A practical characterisation ideally should be a quantity indicative of source strength and involve source factors only. At the same time, it should be in a form appropriate for combining with receiver factors in predicting sound transmission in installed conditions.

This paper considers the case of mechanical installations in buildings. These include, for example, electric motors, compressors, air-handling units and any active component, which generates significant structure-borne sound. Domestic appliances also can be included. The devices nearly always are installed in contact with plate structures such as heavyweight homogeneous structural floors and walls, or floating

floor systems, or stiffened cavity constructions. The range of values of receiver mobility therefore is large and this also must be considered in a practical source characterisation.

The main motivation for the work reported was to examine how laboratory data, in the form of spatial averages and magnitudes, might be used for prediction of installed structure-borne power. As with any simplifying approach, discrepancies between the exact and approximate installed power can be expected. An important outcome of this or any similar study therefore is an assessment of discrepancies and of the acceptability or otherwise of the approximate methods for prediction.

The paper continues by briefly revisiting the theory of structure-borne sound transmission from an active source into a passive receiving system, with an emphasis on the relationship between the source and receiver mobility. A two-stage reception plate method is proposed, the first stage of which yields the source activity in the form of a free velocity term. The second stage yields the source mobility. Both quantities are required for the approximate estimate of the installed power. Case studies are given, based on measured source data and measured and numerically modelled receiver data and the assumptions contained in the two-stage reception plate approach are explored.

2. STRUCTURE-BORNE SOUND TRANSMISSION

Internal mechanisms, impacts, rotations, pressure variations, friction, etc., generate vibrations, which manifest as alternating forces and velocities at the contacts with the supporting and surrounding receiving structures. It is assumed that the source is linear and the internal mechanisms are unaffected by the contact conditions. This ‘black

box' model is implicit in most previous studies of source characterisation and is assumed here [7]. The map of the internal mechanisms, to the external velocities or forces, can be termed the *activity*. Source activity can be expressed as the free velocity v_{sf}, the velocity of the freely suspended source, or the blocked force F_b, the force at the contact with an inert receiver. Direct measurement of free velocity and blocked force usually requires the source to be removed from the installation whilst operating in otherwise normal conditions. There are practical difficulties in duplicating the operating loads on the machine and motors and gearboxes, when they are strongly coupled, for example, into a power train and cannot be treated separately [8]. On the other hand, there are situations that offer the possibility of relatively easy direct measurement, such as for resiliently mounted machines [9] but, in general, there are computational difficulties in calculating these quantities from measurement of contact velocity or force [10]. However, whether or not they can be measured directly, free velocity and blocked force are important concepts, intrinsic to the source, and free velocity in particular will form the basis of the following discussion.

The complex power transmitted to a receiving structure due to a single component of excitation at a contact point is given by [11]

$$W = \frac{1}{2} F^* v \tag{1}$$

F^* is the complex conjugate of the contact force and v is the contact velocity. The following discussion concerns the real part of the complex power $P = Re\ (W)$ since it equates to the flow of energy into the receiving system, which ultimately determines

the far-field radiated sound. The power can be expressed in terms of the free velocity v_{sf} of the source and the complex source mobility Y_S and receiver mobility Y_R [12],

$$P = \frac{1}{2}\left|v_{sf}\right|^2 \frac{Re(Y_R)}{\left|Y_S + Y_R\right|^2} \tag{2}$$

Two complex quantities (Y_S, Y_R) and one real quantity ($\left|v_{sf}\right|$) are therefore required to predict the power in the installed condition.

3. MOBILITIES OF BUILDING INSTALLATIONS

This paper is primarily concerned with the applicability of source data, obtained in the laboratory, in predicting the structure-borne power when the source is installed in buildings. In figure 1 are shown typical values of the magnitude of point mobility of building elements [13], along with values of two sources, at a mount point of a fan unit and at the mount point of a whirlpool bath. In heavyweight buildings the magnitude of the source mobility generally significantly exceeds that of the receiver mobility. In lightweight building constructions, such as timber-frame walls and timber joist floors, the mobility magnitude of the building elements may be greater than, less than or of the same order as that of the source.

For the case of lightweight machines on/in heavyweight structures, common in buildings, the condition $|Y_S| >> |Y_R|$ applies and equation (2) reduces to

$$P \approx \frac{1}{2}\frac{\left|v_{sf}\right|^2}{\left|Y_S\right|^2} Re(Y_R) = \frac{1}{2}\left|F_b\right|^2 Re(Y_R) \tag{3}$$

where F_b is the blocked force i.e. the force at the contact with an inert receiving structure. The installed power then is obtained from it in combination with the receiver mobility, which can be measured or estimated [14, 15].

Conversely, for the case of a rigid machine attached to a flexible structure, $|Y_R| >> |Y_S|$ and equation (2) reduces to

$$P \approx \frac{1}{2}\left|v_{sf}\right|^2 \frac{Re(Y_R)}{\left|Y_R\right|^2} = \frac{1}{2}\left|v_{sf}\right|^2 Re(\frac{1}{Y_R^*}) \qquad (4)$$

The contact velocity is independent of location and a measure of the free velocity only is required to describe the source.

When the ratio of receiver and source mobility lies within the range $0.3 < |Y_R/Y_S| < 3$, a matched mobility condition is of relevance. A detailed discussion of the possible forms of matching is contained in [6], including when the source and receiver mobilities are complex conjugate, $Y_R = Y_S^*$, or a mirror condition when the real parts and imaginary parts are respectively, equal. In addition, a characteristic power also has been proposed, which is the product of the blocked force and free velocity. For a single point of contact, the characteristic power is the same as the source descriptor, previously developed by Mondot and Petersson, to consider single components and points of excitation [12].

In figure 1, some of the source and receiver mobilities display similar behaviour in the matched region (see fan unit and whirpool bath and plasterboard stud between 160 Hz and 500 Hz) and a mirror condition can be assumed. For the mirror condition, equation (2) becomes,

$$P_{mirror} = \frac{1}{8}\left|v_{sf}\right|^2 Re(\frac{1}{Y_S}) = \frac{1}{8}\left|v_{sf}\right|^2 Re(\frac{1}{Y_R}) = \frac{1}{8}\left|v_{sf}\right|^2 \frac{Re(Y_R)}{\left|Y_R\right|^2} \quad (5)$$

4. MULTIPLE CONTACT MULTIPLE COMPONENT SOURCES

Machines and machine components are connected to supporting structures through multiple points, line and area contacts. At each contact, up to six components of excitation and response are possible (three translations and three rotations) and in general there are dynamic interactions between the different contacts and components. The single component and contact expression for complex power becomes

$$W = \frac{1}{2}\left(\{v_{sf}\}^T \left[([Y_S]+[Y_R])^T\right]^{-1}\left[Y_R^*\right]\left[Y_S^*\right]+\left[Y_R^*\right]^{-1}\{v_{sf}^*\}\right) \quad (6)$$

$\{v_{sf}\}$is the free velocity vector and $[Y_{S,R}]$ the mobility matrices. For N contacts, a 6Nx6N mobility matrix is required. For example, it is possible to assemble the terms required for the characteristic power,

$$W = \frac{1}{2}\left(\{v_{sf}\}^T \left[(Y_S)^T\right]^{-1}\{v_{sf}^*\}\right) \quad (7)$$

The characteristic power simplifies the representation of source strength as a single spectrum, but the full free velocity and source mobility sets still are required for this and other source characterisations [6,16].

An alternative laboratory reception plate approach, proposed in this paper, stems from the following observations. The first is that most receiver structures in

buildings are plate-like in dynamic behaviour. Thus a laboratory (reception) plate can be constructed with a dynamic behaviour which approximates that of the real installed condition or which generates laboratory data easily transformed into a prediction of the installed condition. When the machine of interest is attached to a simple reception plate, the structure-borne sound transmission, through all contacts and components of excitation, can be rendered down to a single value, since it is equal to the reception plate bending wave power. The reception plate power is obtained from the mean square plate velocity, the total loss factor and mass of the plate. All these quantities are easily measurable [17].

Secondly, the main components of source excitation, which excite the reception plate into bending vibration, are likely to be the same as for the real installed condition. The source mechanisms dictate whether forces or moments dominate the transmission and moments should not be neglected a priori. However, from previous studies of sources in heavyweight buildings, forces perpendicular to the receiving plate structure generally dominate the structure-borne transmission [18].

Thirdly, the characteristic mobility approximates the mobility of floors and walls at mid and high frequencies. The low frequency modal behaviour can be addressed by assigning an upper and lower limit to the mobility according to Skudrzyk [19, 20]. It is relatively straightforward to calculate the characteristic and limiting values from the plate dimensions, material and loss factor.

Fourthly, data reduction will result by reference to the concept of the effective mobility, used to preserve the clarity of the single point single component representation of equation (6) [21, 22]. The concept is based on the premise that the power can be estimated at each contact but where the influence of all other contacts (and components) is included. The total power is then the sum of all contact powers.

For a machine with N contacts with a floor and where perpendicular forces are dominant, the effective point mobility at the *ith* contact can be written as,

$$Y_i^{\Sigma} = Y_i + \sum \frac{F_j}{F_i} Y_{i,j} \tag{8}$$

Y_i is the point mobility at the ith contact, $Y_{i,j}$ is the transfer mobility between the ith and jth contacts and $\frac{F_j}{F_i}$ is the ratio of the forces at the jth and ith contact, respectively. Equation (8) reveals a requirement for the force distribution $\frac{F_j}{F_i}$ at the contacts and therefore of the dynamics of both the receiver and source structures. In the absence of detailed knowledge of the contact forces, the forces can be assumed to be of equal magnitude, with either zero phase difference between contact forces, or with a random phase difference [23]. If a zero phase difference is assumed, then equation (8) becomes,

$$Y_i^{\Sigma} \approx Y_i + \sum Y_{i,j} \tag{9}$$

If a random phase is assumed [21, 22] then,

$$\left|Y_i^{\Sigma}\right|^2 \approx \left|Y_i\right|^2 + \sum \left|Y_{i,j}\right|^2$$

and

$$\mathrm{Re}\left(Y_i^{\Sigma}\right) \approx \mathrm{Re}\left(Y_i\right) \tag{10}$$

5. TWO-STAGE RECEPTION PLATE METHOD

In proposing a laboratory-based measurement method for mechanical installations in buildings, it is recognised that manufacturers generally require methods, which yield a single value of source strength, even if there is some loss of accuracy and not all situations are amenable to the approach. The approach presently proposed is based on the reception plate, the theory of which is given in [11] and a practical implementation is described by Lu et al [24].

The present proposal is a development in that the installed source-receiver mobility conditions are approximated in the laboratory. Two stages are required to obtain the free velocity and source mobility terms in separable form. The development stems from experimental work conducted by Späh et al [25] in which a 100mm concrete plate was resiliently mounted as a reception plate. On it was mounted the source for test. It was recognised that the plate could not be assumed to be providing a diffuse bending wave field condition (with high modal overlap factor) as required by [11] but it was demonstrated that it was possible to compensate for the low frequency modal behaviour of the receiver plate by assigning upper and lower limits [20] to the mobility.

Essentially, the approach is to approximate two installation conditions, in the laboratory, corresponding to the asymptotic conditions, shown in Figure 2: a blocked force approximation when $|Y_R| << |Y_S|$ and a velocity source approximation when $|Y_R| >> |Y_S|$. The approach to predicting the power in the installed condition then is to explore whether either of the asymptotic conditions is appropriate, or if a matched mobility condition can be invoked.

Consider a source connected through multiple (N) contacts to a series of supporting plate structures similar to Figure 2. In this study, forces perpendicular to the receiver plate only are considered. The power through the ith contact is obtained from equation (2) but where point mobility terms are replaced with effective mobilities (see equations (8)-(10)),

$$P_{SRi} = \frac{1}{2}\left|v_{sfi}\right|^2 \frac{\mathrm{Re}(Y^{\Sigma}{}_{Ri})}{\left|Y^{\Sigma}{}_{Si} + Y^{\Sigma}{}_{Ri}\right|^2} \tag{11}$$

The total power through N contacts is,

$$P_{SR}^{Total} = \frac{1}{2}\sum_{i}^{N}\left|v_{sfi}\right|^2 \frac{\mathrm{Re}(Y^{\Sigma}{}_{Ri})}{\left|Y^{\Sigma}{}_{Si} + Y^{\Sigma}{}_{Ri}\right|^2} \tag{12}$$

If the source under test is placed on a low mobility plate *R*, where $\left|Y_{Si}^{\Sigma}\right| >> \left|Y_{Ri}^{\Sigma}\right|$ for all i, the total structure-borne power becomes,

$$P_{SR}^{Total} \approx \frac{1}{2}\sum_{i}^{N} \frac{\left|v_{sfi}\right|^2}{\left|Y^{\Sigma}{}_{Si}\right|^2}\mathrm{Re}(Y_{Ri}^{\Sigma}) \tag{13}$$

If it is assumed that,

$$\sum_{i}^{N} \frac{\left|v_{sfi}\right|^2}{\left|Y^{\Sigma}{}_{Si}\right|^2}\mathrm{Re}(Y_{Ri}^{\Sigma}) \approx \frac{1}{N}\sum_{i}^{N} \mathrm{Re}(Y_{Ri}^{\Sigma})\sum_{i}^{N} \frac{\left|v_{sfi}\right|^2}{\left|Y^{\Sigma}{}_{Si}\right|^2} = \mathrm{Re}(Y_{R}^{\Sigma})\sum_{i}^{N} \frac{\left|v_{sfi}\right|^2}{\left|Y^{\Sigma}{}_{Si}\right|^2}$$

Equation (13) becomes

$$P_{SR}^{Total} \approx \frac{1}{2}\mathrm{Re}(Y_R^{\Sigma})\sum_{i}^{N} \frac{\left|v_{sfi}\right|^2}{\left|Y^{\Sigma}{}_{Si}\right|^2} \qquad (14)$$

This condition is met, for example, if $\mathrm{Re}(Y^{\Sigma}{}_{Ri}) = \mathrm{Re}(Y^{\Sigma}{}_{Rj}) = \mathrm{Re}(Y_{Rk}{}^{\Sigma}) = ... = \mathrm{Re}(Y_R{}^{\Sigma})$

In Figure 3 is shown the real part of the measured effective mobility $\mathrm{Re}(Y_R{}^{\Sigma})$ at four contact points on a resiliently supported free plate of 100mm concrete of area 2.8m x 2.0 m. The real part of the effective mobility is calculated, as one third octave values, from equation (8) for a tested whirlpool bath where the complex contact forces were obtained from measured free velocities and source and receiver mobilities. The range of values is of the order of 10 dB and is the result of variation in contact force over the four positions. Results, presented in Figure 4, are for an assumed unit force ratio and zero phase difference. Values of $\mathrm{Re}(Y_R{}^{\Sigma})$ can be obtained from measured point and transfer mobilities on the laboratory reception plate, as an average or a typical value and this can serve for all machine installations on the plate.

The total structure-borne power transmitted is obtained from the spatial average of the mean square plate velocity $\left\langle v_R^2 \right\rangle$ according to [11], as

$$P_{SR}^{Total} = \omega \eta_R \ddot{m}_R S_R \left\langle v_R^2 \right\rangle \qquad (15)$$

η_R is the total loss factor of the receiving plate of area S_R and $\ddot{m}$ mass per sq. metre.

The right hand sides of equations (14) and (15) equate and all terms on the right hand side of (15) are measurable, along with Y_R^{Σ} in (14). The value $\sum_i^N \frac{\left|v_{sfi}\right|^2}{\left|Y^{\Sigma}{}_{Si}\right|^2}$ is obtained, equivalent to the blocked force representation $\sum_i^N \left|F_{bi}\right|^2$.

Repeating the process for the source now attached to a high mobility plate *R'*, where $\left|Y_{Si}^{\Sigma}\right| << \left|Y_{Ri'}^{\Sigma}\right|$, then equation (12) becomes

$$P_{SR'}^{Total} \approx \frac{1}{2}\sum_i^N Re\left(\frac{1}{(Y^{\Sigma}{}_{R'i})}\right)\left|v_{sfi}\right|^2 = \frac{1}{2}\frac{1}{N}\sum_i^N Re\left(\frac{1}{(Y^{\Sigma}{}_{R'i})}\right)\sum_i^N \left|v_{sfi}\right|^2 \qquad (16)$$

and

$$P_{SR'}^{Total} \approx \frac{1}{2} Re\left(\frac{1}{Y^{\Sigma}{}_{R'}}\right)\sum_i^N \left|v_{sfi}\right|^2 \qquad (17)$$

The term outside the summation can be obtained from laboratory measurement and the sum of the squares of the free velocities at the contacts $\sum_i^N \left|v_{sfi}\right|^2$ is obtained. In Figure 5 is shown the calculated real part of the effective mobilities for four contact points, corresponding to the four support points of the whirlpool bath, on a high mobility plate, a reception plate of 3mm aluminium. In Figure 6 is shown the calculated real part of the effective mobilities for four contact points, corresponding to the four support points of a medium size fan unit, on the same 3mm aluminium plate. In Figure 7 is shown values where a unit force ratio, zero phase difference, is

assumed. In Figure 8 are shown the corresponding values $\mathrm{Re}(\frac{1}{Y^{\Sigma}_{R'}})$. The range of values is of the order of 3 dB for frequencies above 100 Hz.

Can this approach be taken further to obtain the average effective source mobility $\left|Y_S^{\Sigma}\right|$ from equations (14) and (17)? This is possible if the effective source mobilities at each source contact are assumed the same. The source mobilities of machines and appliances generally are more complicated functions of frequency than the simple laboratory plate receiver systems so far described and spatial variations in the dynamics of the contacts is likely to be greater. However, machines often are of a symmetric geometry and support conditions are repeated (although this should not be generally assumed). In Figures 9 and 10 are values of $\left|Y_S^{\Sigma}\right|$ at the support points of the fan base and whirlpool bath, respectively. If the values at the four contacts are assumed the same, then equation (14) becomes,

$$P_{SR}^{Total} \approx \frac{1}{2}\mathrm{Re}(Y_R^{\Sigma})\frac{1}{\left|Y_S^{\Sigma}\right|^2}\sum_{i}^{N}\left|v_{sfi}\right|^2 \qquad (18)$$

From equations (17) and (18) the average magnitude of the effective source mobility $\left|Y_S^{\Sigma}\right|$ is obtained.

6. CASE STUDIES

In the following case studies, the proposed two-stage laboratory procedure is simulated using measured source data and numerically modelled reception plates. The two sources considered are again the fan unit and the whirpool bath. In each case, the

measured source data consisted of 4 free velocity spectra and 4x4 point and transfer mobility spectra. The laboratory reception plates are modelled, as before, as free (FFFF) plates: a 3mm aluminium plate and a 100mm concrete plate. The floor for the installed condition was modelled as a simply supported (SSSS) plate of material and thickness selected to ensure different source-receiver mobility conditions occur over the frequency range of interest. Plate point and transfer mobilities were combined with the source data to yield an exact value of the installed powers (as narrowband or one third octave values) for comparison with the approximate predictions, which used the reception plate data, available as one third octave values. Again, a unit force, zero phase condition was assumed in the calculation of effective mobility.

In figures 11 and 12 are shown the sum of the squared free velocities $\sum_{i}^{N} \left|v_{sfi}\right|^2$ for the fan unit and whirlpool bath, respectively. Directly measured values are compared with reception plate values, obtained from equations (15) and (17), when the sources are mounted in the 3mm aluminium plate. The reception plate values are within 5 dB of the true values for the whirpool bath and within 5 dB for the fan unit at frequencies above 200 Hz. For the fan, the larger discrepancy below 200 Hz, results from a combination of plate modal behaviour and small distances between mount points, leading to interference effects.

In figures 13 and 14 are shown the average magnitude of the source effective mobility $\left|Y_S^{\Sigma}\right|$ for the same sources. Directly measured values are compared with reception plate values, obtained from equations (15), (17) and (18) when the sources are mounted on the 3mm aluminium plate and then on the 100 mm concrete plate. The reception plate values are within 5 dB of the true values for both cases except at 100

Hz for the fan, where the source mobility at the anti-resonance is approaching that of the reception plate, which itself could be resonant.

Now consider an installed condition, the fan unit on a 50mm homogeneous timber floor, of area 4.5 m x 4m. This case provides a bench marking exercise and does not correspond to a real timber floor construction, which would normally include wooden beam supports.

The first step in estimating the installed power, using the reception plate data, is to compare source and receiver effective mobilities. The source effective mobility is that shown in figure 13. The receiver mobility is estimated from the characteristic mobility [11],

$$Y_{char} = \frac{1}{8\sqrt{B'\ddot{m}}} \tag{19}$$

where *B'* is the bending stiffness. An effective mobility can be obtained, in simplest form, by assuming a unit force distribution and that transfer mobilities are equal to the point mobilities at low frequencies. Equation (9) becomes,

$$Y_R^{\Sigma} \approx 4Y_{char} \tag{20}$$

At high frequencies, the transfer mobilities terms reduce, relative to the point mobilties, and equation (9) becomes,

$$Y_R^{\Sigma} \approx Y_{char} \tag{21}$$

The transition from low to high frequency condition can be assumed to occur when the Helmholtz number $k_b r = 1$. k_b is the bending wavenumber and *r* is a representative distance between contact points. For the fan considered, the Helmholtz number has

unit value in the 160 Hz band. Shown in figure 15 are the approximate values of magnitude of effective mobility of the floor, from equations (19) – (21). Also shown is the exact value for the known force distribution and for an assumed unit force ratio and zero phase difference.

In figure 16, the source and receiver effective mobility magnitudes are compared (again, only the approximate estimates of receiver mobility are assumed available from equations (19) – (21)). Three conditions are identified. In the frequency range 50 - 125 Hz equation (4) is used, where point mobility is replaced with effective mobility. At 160 Hz, equation (5) is used. In the frequency range 200 Hz – 1000 Hz equation (3) is used. In figure 17 the exact value of installed power is shown with the approximate values in the three frequency regions. The exact value was calculated using narrow band complex values and then converted to one third octave values. The approximate value was calculated using third octave values throughout. The agreement between the approximate and exact values is promising in the mid and high frequencies. The discrepancies at low frequencies are the result of assuming infinite plate behaviour for the floor when a modal behaviour is evident.

7. PRACTICALITIES OF TWO-STAGE RECEPTION PLATE METHOD

A low mobility reception plate has been constructed of concrete of dimensions 2.8 m by 2.0 m and a thickness of 100 mm in the laboratories of Stuttgart University of Applied Science [26]. This allows a high mobility source assumption. It has been confirmed that the laboratory reception plate power can be transformed into an installed power for concrete floors in buildings by consideration of the ratio of floor and reception plate mobility. The method provides laboratory data which can be

transformed into input data for predictions of sound pressure level from mechanical installations in heavyweight buildings [27, 28].

A high mobility reception plate could be fabricated from thin metal sheet or other thin building material, such that the point mobility is 10dB greater than that of the source to be tested. It could have free edges or be attached to a supporting frame and should be of an area to provide high modal overlap and sufficient room for attachment of the accelerometers. A plate of 3mm aluminium of dimensions, 3m x 2m, should be sufficient, although large machines may require a greater area of plate. Such plates would not be required to serve a structural purpose. The source for testing would be mounted onto the plate, which in turn would be supported by soft mounts directly below the contacts with the source. This would provide sufficient static support and, at the same time, give the required mobility condition $|Y_{mount}| >> |Y_{R'}| >> |Y_S|$. Damping could be introduced to increase modal overlap factor and reduce spatial variation in plate velocity as required. The practicalities of this test plate have yet to be considered.

9. DISCUSSION AND CONCLUDING REMARKS

A two-stage reception plate method of characterising structure-borne sound sources is proposed for mechanical installations in buildings. The first stage yields the sum of the square velocities over the source contacts. The second stage yields the average of the magnitude of the effective mobility over the same source contacts. The free velocity also can be measured directly for machines supported at few contacts, again as the sum of the squared values. However, the reception plate method offers advantages of simplicity when measuring the free velocity at many contact points or

when many similar machines have to be measured. The method applies to line and area contacts. In this case, the contacts can be discretised and values assigned to the linear array or mesh.

It is unlikely that floor and wall mobilities will be measured prior to predicting the structure-borne power from machines to be installed. However, early and often acceptable estimates of receiver effective mobility are possible, for homogeneous floors, based on the characteristic mobility (the assumed mobility of an infinite plate of the same thickness and material as the real plate). Lightweight building elements are of frame and cavity construction and the point mobility will vary significantly with location. The concept of an average effective mobility is more tenuous and this should be explored in further case studies..

So far, perpendicular force excitations have been considered and it remains to include the effect of other components of excitation, particularly moments, and this should be possible by reference to the expanded form of the effective mobility.

The method proposed, as with most simplified methods, is a trade-off between practical application and accuracy. The practical benefits of a reception plate method are clear. The laboratory measurement data generated is in simple and transferable form. Manufacturers could check the efficacy of various vibration control stratagems, such as the introduction of anti-vibration mounts, by repeat measurements.

ACKNOWLEDGEMENTS

The authors gratefully acknowledge the contributions of Moritz Späh and Heinz-Martin Fischer of Stuttgart University of Applied Science, of Werner Scholl, Physikalisch-Technische Bundesanstalt (PTB), Braunschweig, and Michel Villot of

CSTB, Grenoble, for their advice during discussions, and for measurement data, included in this paper. The authors also acknowledge the financial support of the Engineering and Physical Sciences Research Council of the U.K.

REFERENCES

1. Bodén, H., *Characterisation of fluid-borne and structure-borne sound sources*, 9th International Congress on Sound and Vibration, 1-30, Florida (2002).
2. Ohlrich, M., *Structure-borne sound sources and their power transfer*, Proc. Internoise 2000, pp 11, The Hague (2001.)
3. ten Wolde, T., Gadefelt, T.G.R., *Development of standard methods for structure-borne sound emission,* Noise Control Engineering Journal, 28, 5-14 (1987). Note Errata in 28, 84 (1987).
4. Verheij, J.W., *Inverse and Reciprocal Methods for Machinery Noise Source Characterization and Sound Path Quantification,* International Journal of Acoustics and Vibration, vol. 2(1), 11-20 (1997).
5. Petersson, B.A.T., Gibbs, B.M., *Towards a structure-borne sound source characterization,* Applied Acoustics, 61, 325-343 (2000).
6. Moorhouse, A.T., *On the characteristic power of structure-borne sound sources,* Journal of Sound and Vibration 248(3), 441-459 (2001).
7. R*eport from the workshop on source characterisation - Liverpool '96*, Journal of Sound and Vibration, 200, 757-758 (1997).
8. Ohlrich, M., T*erminal source power for predicting structure-borne sound transmission from a main gearbox to a helicopter fuselage,* Proc*. Internoise 95* vol. 1, 555-558 (1995).
9. ISO 9611: 1996 *Characterization of sources of structure-borne sound with respect to sound radiation from connected structures - Measurement of velocity at the contact points of machinery when resiliently mounted.*
10. Mondot J.M. and Moorhouse A.T., *The Characterisation of Structure-borne Sound Sources,* Proc. Internoise 96, 3 1439-1442 (1996).
11. Cremer, L., Heckl, M., and Petersson B.A.T., S*tructure-borne Sound,* 3rd edition, Springer (2005).
12. Mondot, J.M., and Petersson, B.A.T., *Characterisation of structure-borne sound sources: The source descriptor and coupling function,* J. Sound Vib. 114 (3), 507-518 (1987).
13. Scholl, W, *About a test facility for installation noise in wooden houses,* Forum Acusticum,

Budapest, 1977-1981 (2005).

14. Breeuwer, R., and Tukker, J.C. *Resiliently mounting systems in buildings,* Applied Acoustics 9, 77-101, (1976).

15. Moorhouse, A.T., and Gibbs, B.M., *Prediction of the structure-borne noise emission of machines: Development of a methodology,* J. Sound Vib. 167 (2), 223-237 (1993).

16. Su Jian Xin, *Simplified characterization of structure-borne sound sources with multi-point connections*, PhD Thesis, University of Liverpool, (2003).

17. Qi, N, Gibbs, B M, *Structure-borne power from machines in buildings: Prediction of installed power from laboratory measurement,* Forum Acusticum, Budapest, 1901-1905 (2005).

18. Yap S H and Gibbs B M, *Structure-borne sound transmission from machines in buildings, part 2: Indirect measurement of force and moment at the machine-receiver interface of a single point connected system by a reciprocal method,* Journal of Sound and Vibration, 222 (1), 99-113 (1999).

19. Skudrzyk E, *The mean value method of predicting the dynamic response of complex vibrators,* Journal of the Acoustical Society of America, 67, 347- 59, 1981.

20. Moorhouse, A.T. and Gibbs, B.M., *Calculation of the mean and maximum mobility for concrete floors,* Applied Acoustics 45, 227-245, 1995.

21. Petersson, B.A.T., and Plunt, J., *On effective mobilities in the prediction of structure-borne sound transmission between a source and a receiving structure, Part 1: Theoretical background and Basic Experimental Studies Procedures,* J. Sound Vib. 82 (4), 517-529 (1982)

22. Petersson, B.A.T., and Plunt, J., *On effective mobilities in the prediction of structure-borne sound transmission between a source and a receiving structure, Part 2: Estimation of mobilities,* J. Sound Vib. 82 (4), 531-540 (1982).

23. Fulford, R.A. and Gibbs, B.M., *Structure-borne sound power and source characterisation in multi-point-connected systems, Part1: Case studies for assumed force distributions,* J. Sound Vib. 204(4), 659-677 (1997).

24. Lu J, Louvigne B, Pascal J.B , Tourret, J., *The perforated reception plate; a practical method for the characterization of structure-borne noise emitted by small equipment*, Proc. Internoise 90, Vol 1, 217-220 (1990).

25. Späh M., Gibbs B.M., Fischer H-M., *Measurement of Structure-borne Sound Power of Mechanical Installations in Buildings*, 11th International Congress on Sound and Vibration, St Petersburg (2004).

26. Späh M, Fischer H-H, Gibbs B M, *New laboratory for the measurement of structure-borne sound power of sanitary installations,* Forum Acusticum, Budapest, 1907-1912 (2005).

27. Gerretsen, E., *Prediction model for sound transmission from machinery in buildings: Feasible approaches and problems to be solved,* Proc. Internoise 2000, 3345-3350 (2000).

28. EN 12354-5, *Building Acoustics: Estimation of acoustic performance of buildings from the performance of elements, Part 5: Sound levels due to service equipment* (draft 2005).

LEGENDS

Figure 1. Magnitude of point mobility for installations in buildings: sources (solid lines), receivers (dashed lines). Values for plasterboard-timber construction, after [13]

Figure 2. Two-stage laboratory reception system and installed condition

Figure 3. Measured real part of effective mobility at four contact points on a free 100mm concrete plate (2.8 x 2.0 m) with a force distribution corresponding to a tested whirlpool bath

Figure 4. Measured real part of effective mobility at four contact points on a free 100mm concrete plate with an assumed unit force ratio distribution

Figure 5. Calculated real part of effective mobility at four contact points on a free 3mm aluminium plate (3 x 2 m) with a force distribution corresponding to an installed whirlpool bath

Figure 6. Calculated real part of the effective mobility at four contact points on a free 3mm aluminium plate (3 x 2 m) with a force distribution corresponding to a medium size fan unit

Figure 7. Calculated real part of the effective mobility at four contact points on a free 3mm plate with an assumed unit force ratio distribution.

Figure 8. Calculated $\mathrm{Re}(\frac{1}{Y^{\Sigma}{}_{R'}})$ at four contact points on a free 3mm plate, with unit force ratio distribution

Figure 9. Calculated $\left|Y_S^{\Sigma}\right|$ at four contacts of a fan base; unit force ratio assumption

Figure 10. Calculated $\left|Y_S^{\Sigma}\right|$ at four contacts of a whirlpool bath; unit force ratio assumption

Figure 11. Sum of squared free velocities over four support points of a fan unit

Figure 12. Sum of squared free velocities over four support points of a whirlpool bath

Figure 13. Average magnitude of effective source mobility $\left|Y_S^{\Sigma}\right|$ of a fan unit

Figure 14. Average magnitude of effective source mobility $\left|Y_S^{\Sigma}\right|$ of a whirlpool bath

Figure 15. Magnitude of effective mobility of 50mm timber floor: solid line, exact value; light solid line, for unit force ratio and zero phase difference; dashed line, from equations (20) and (21).

Figure 16. Magnitude of effective mobility: solid line, source (fan unit); dashed line, receiver (50mm floor) from equations (20) and (21).

Figure 17. Installed power for a fan unit on a 50mm timber floor: Solid line, exact value: dashed lines, approximate values; circle, matched mobility estimate.

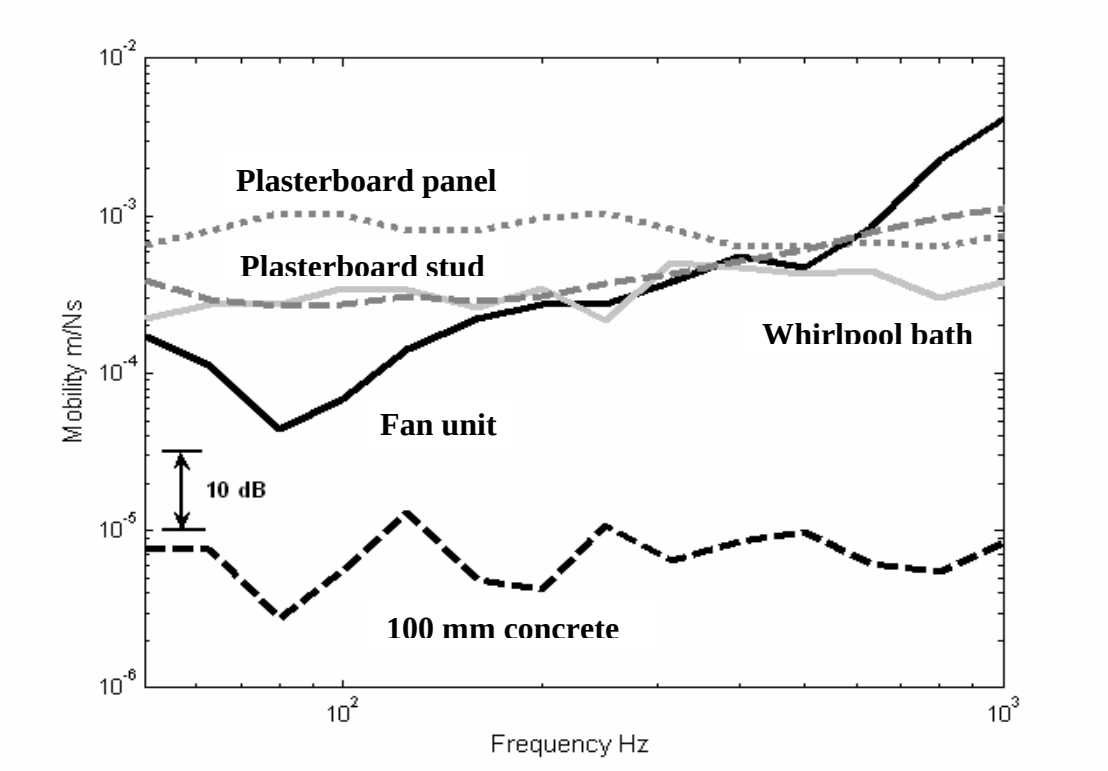

FIGURE 1

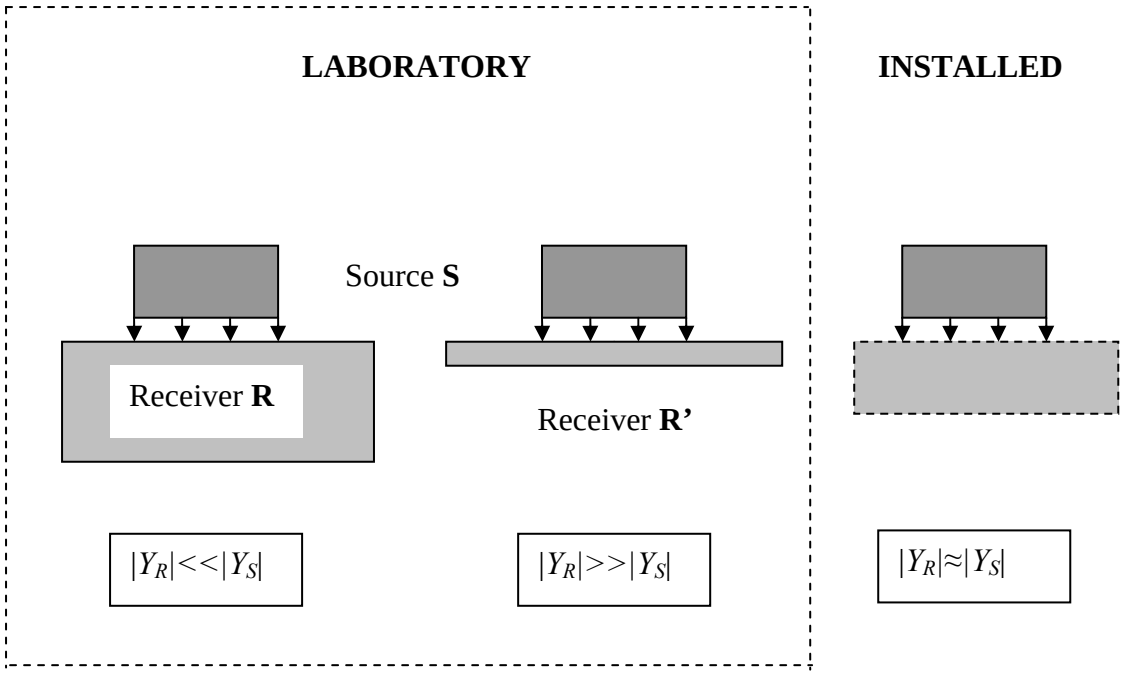

FIGURE 2

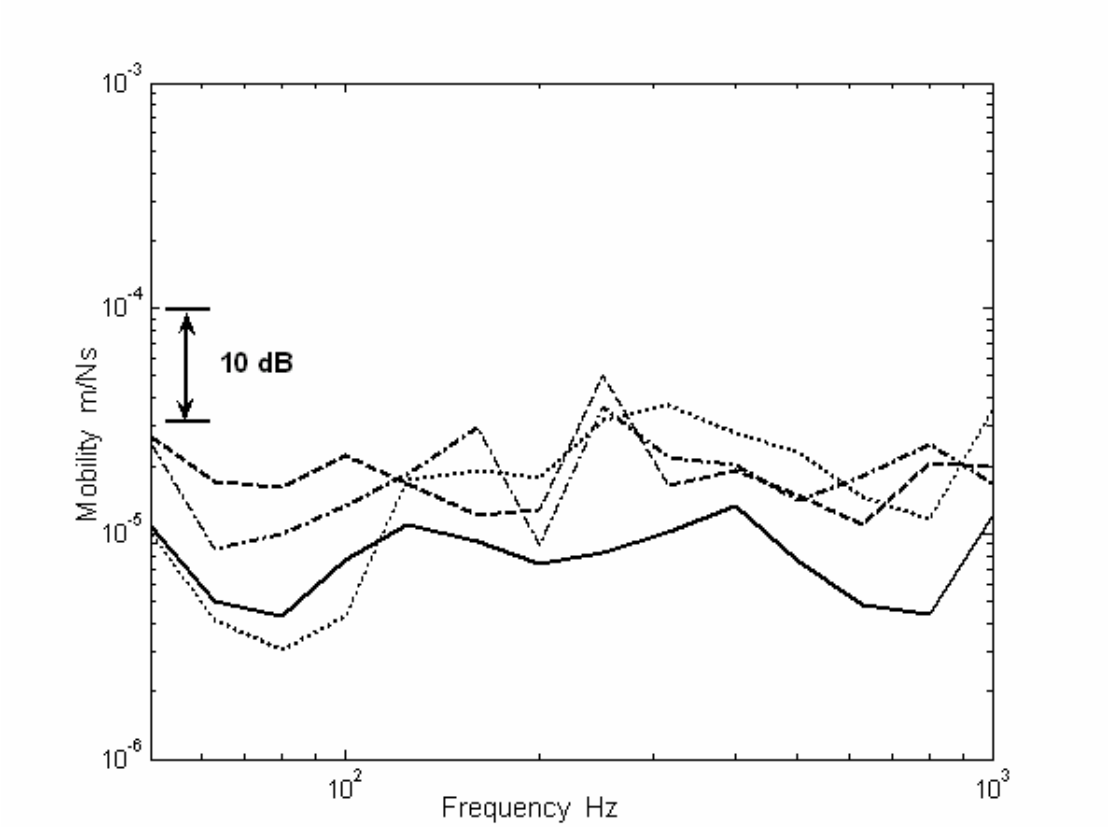

FIGURE 3

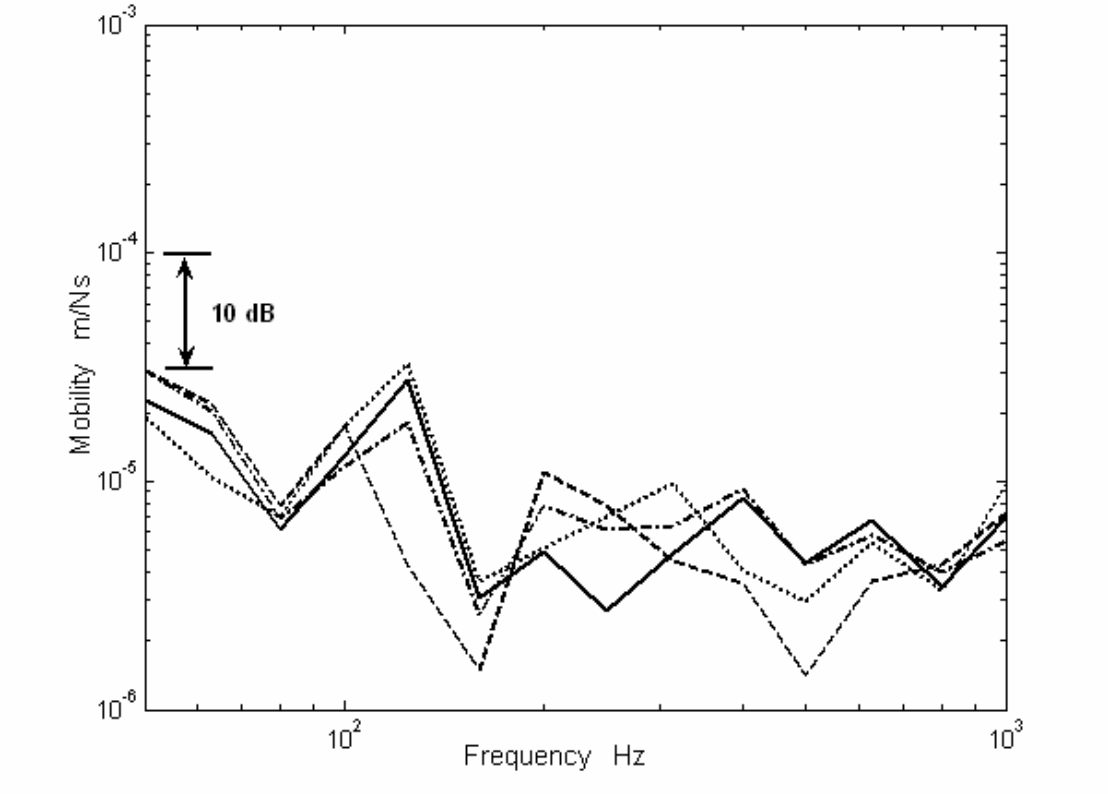

FIGURE 4

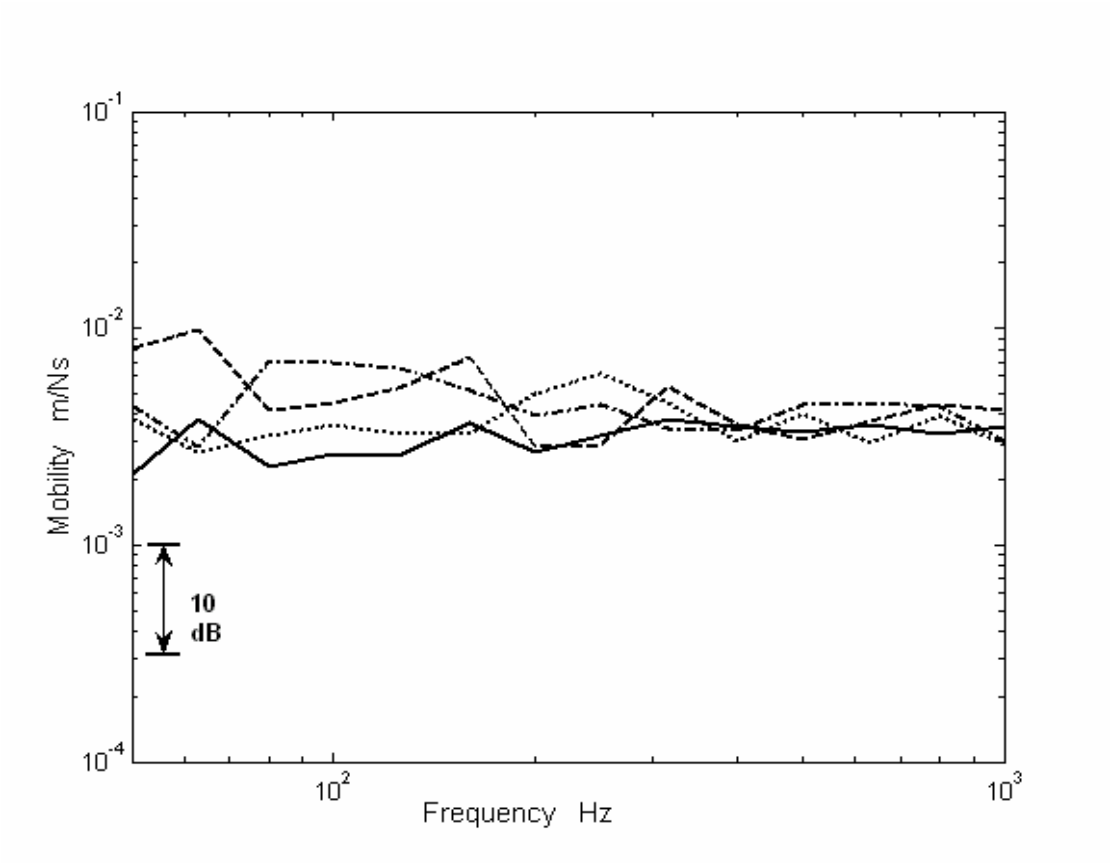

FIGURE 5

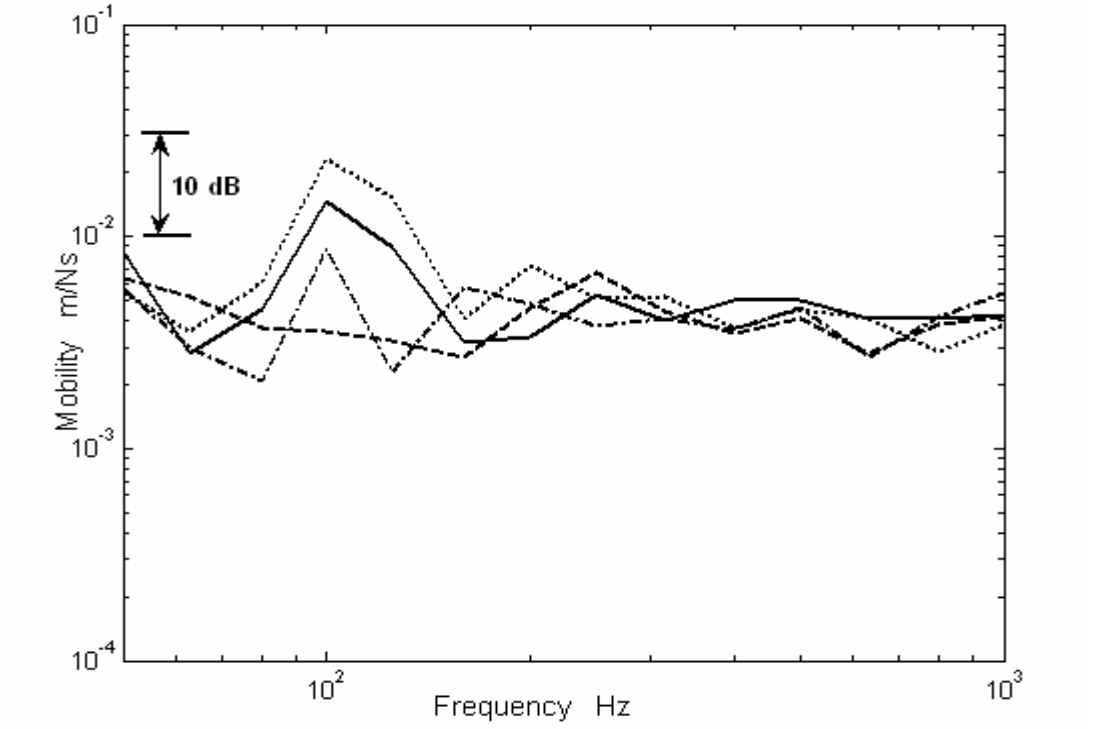

FIGURE 6

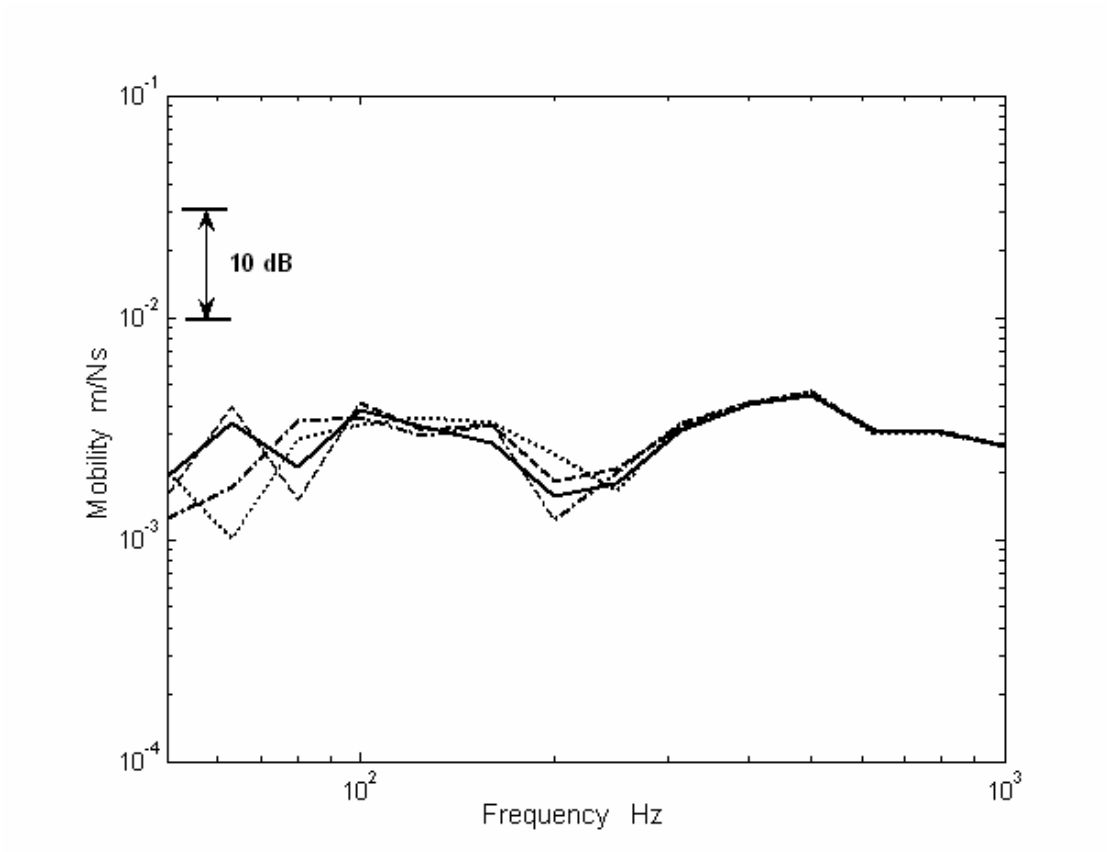

FIGURE 7

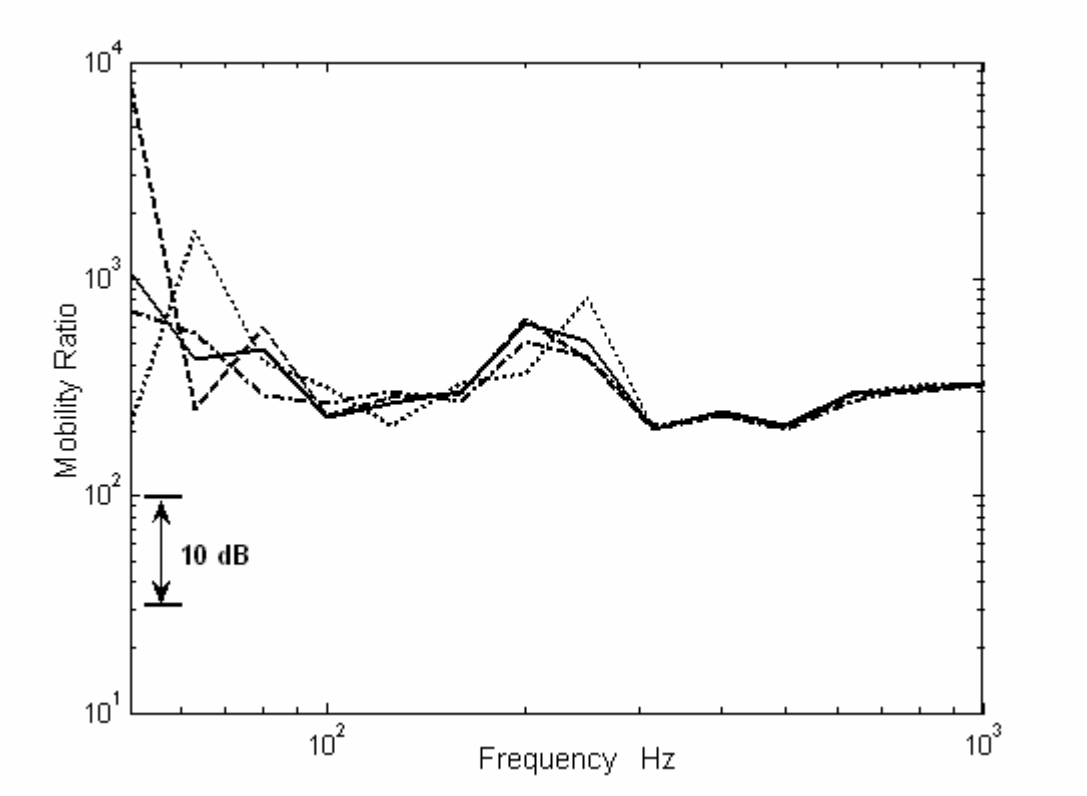

FIGURE 8

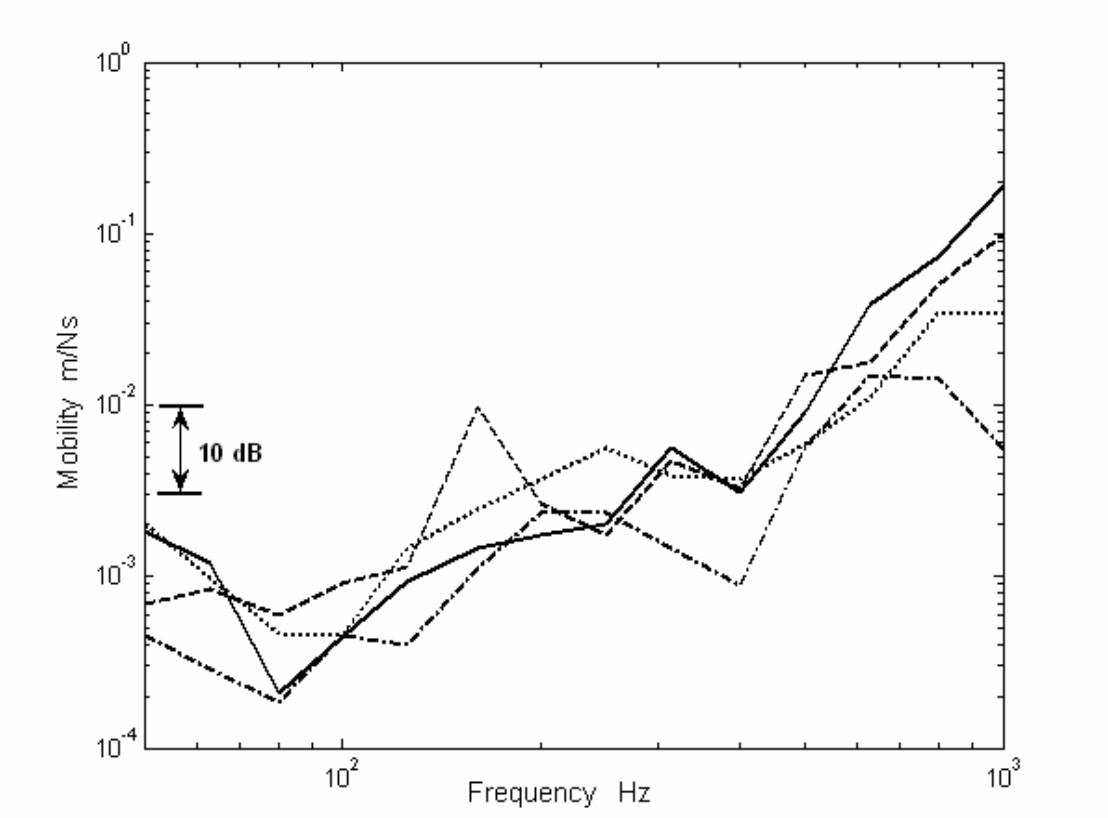

FIGURE 9

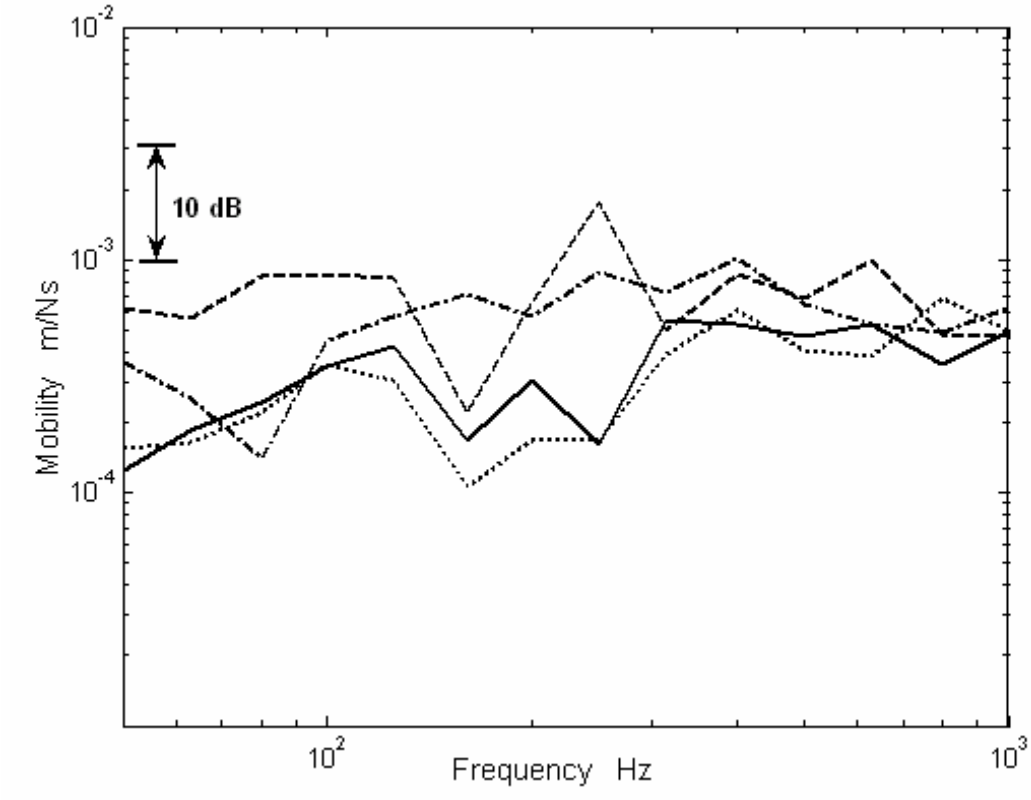

FIGURE 10

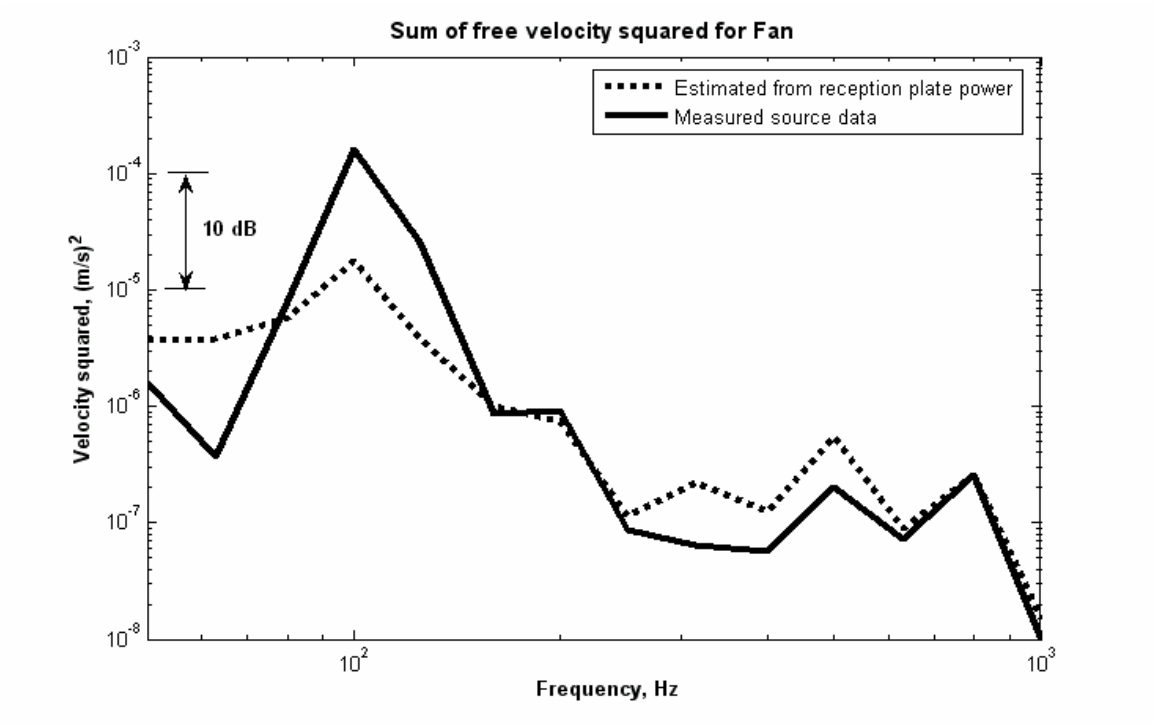

FIGURE 11

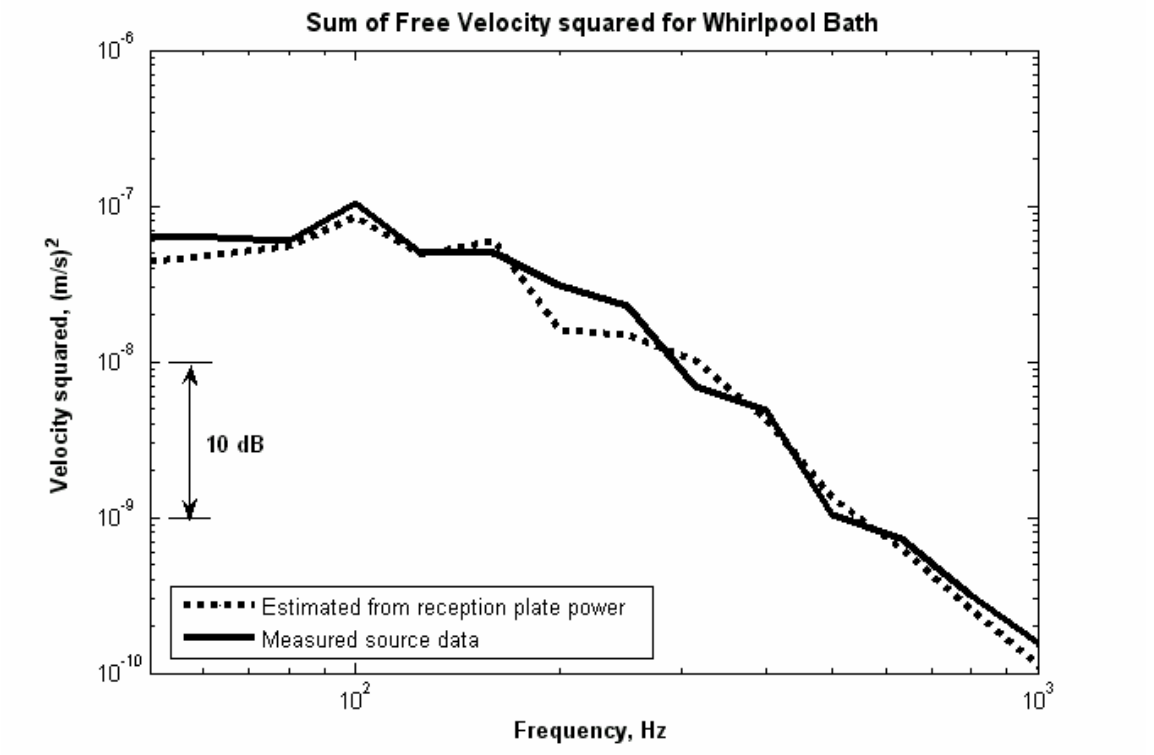

FIGURE 12

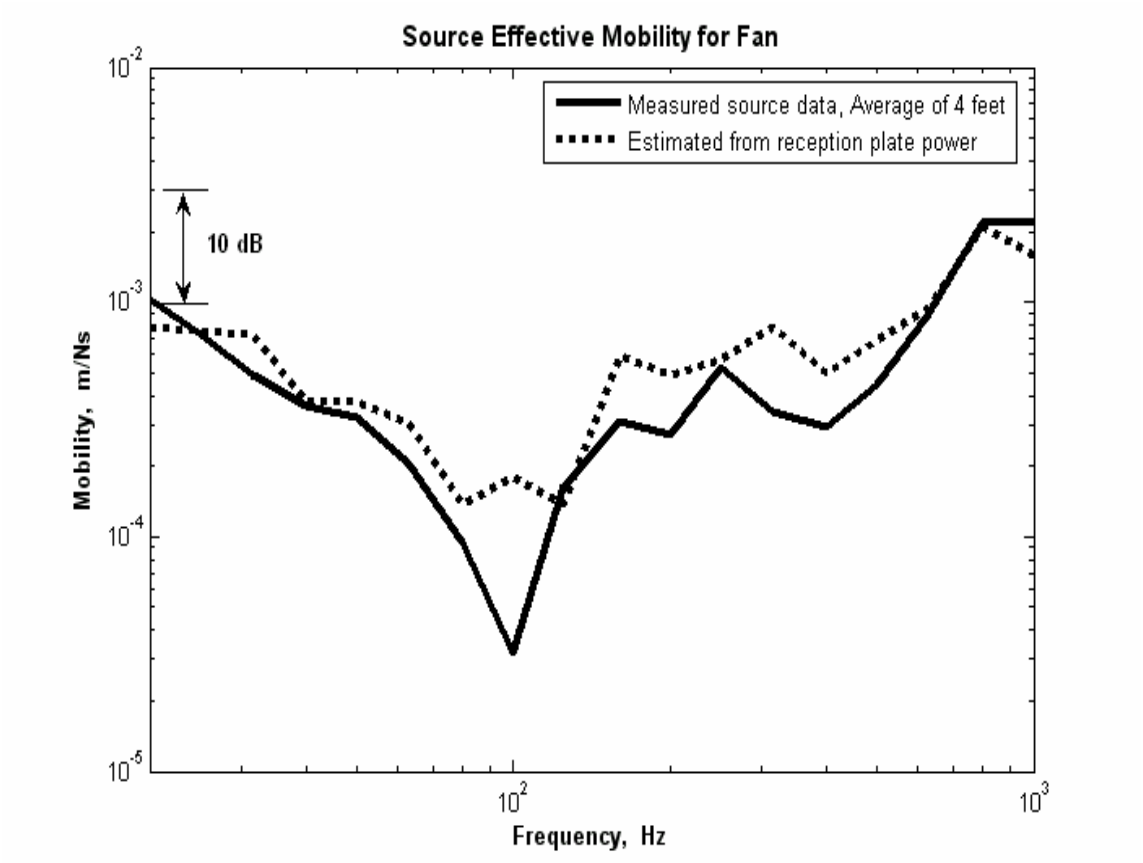

FIGURE 13

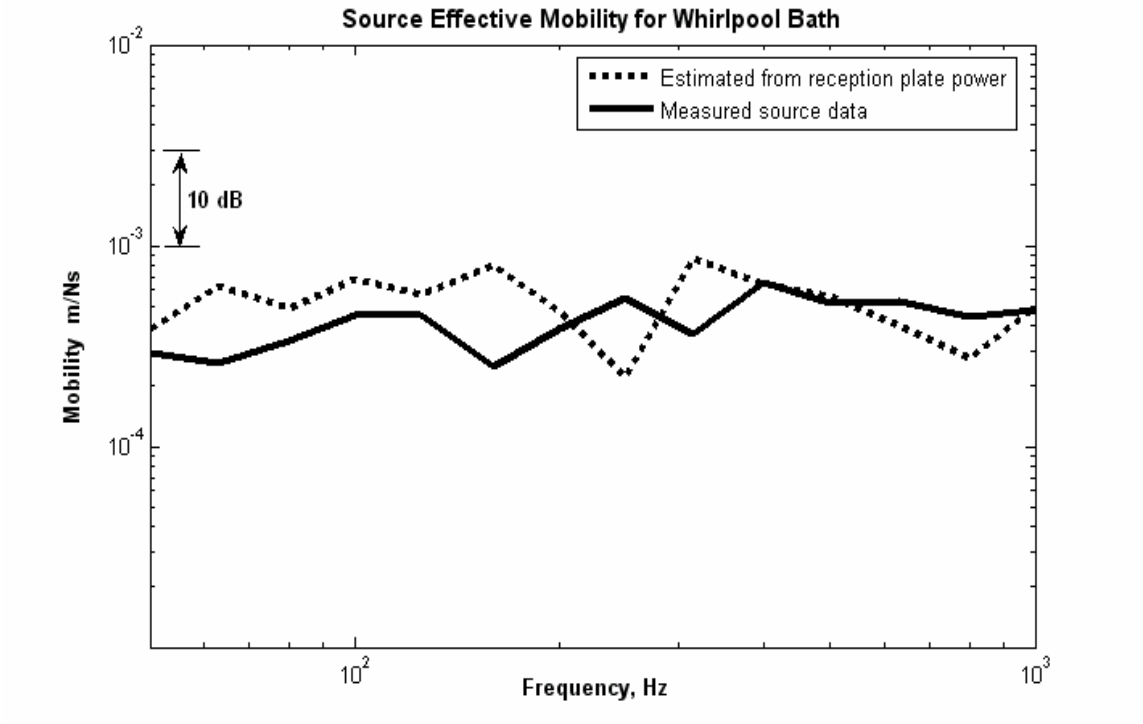

FIGURE 14

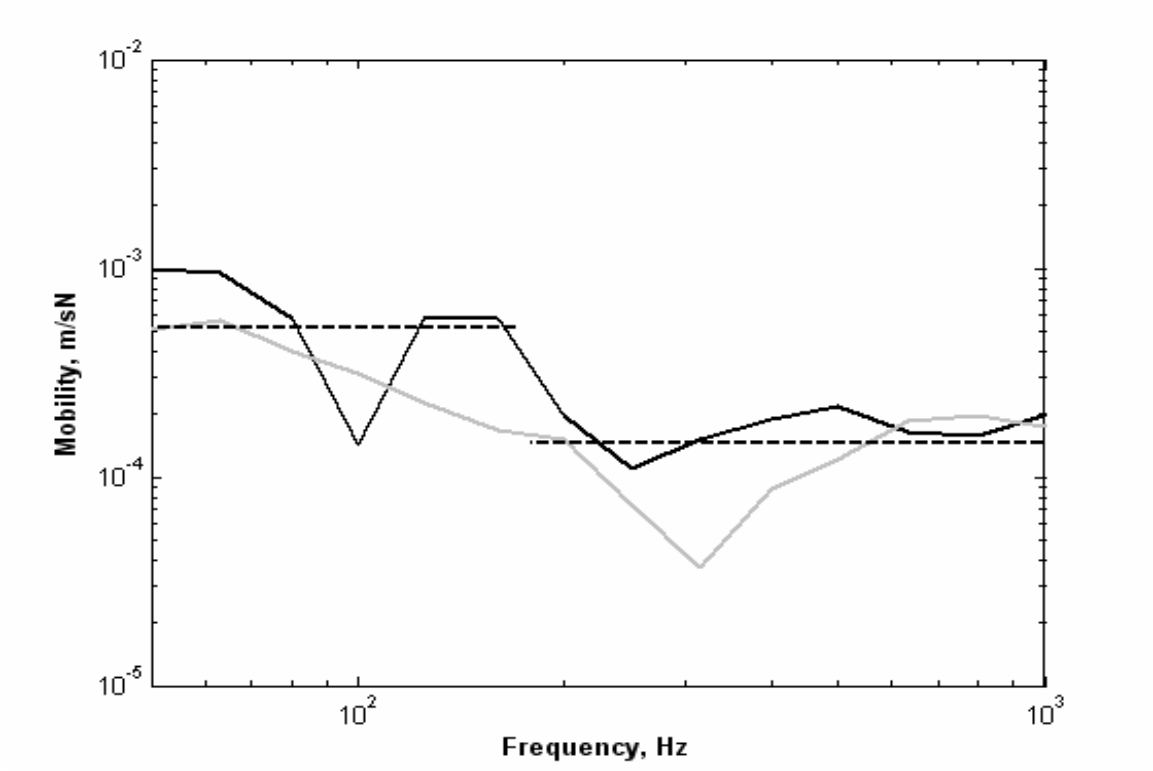

FIGURE 15

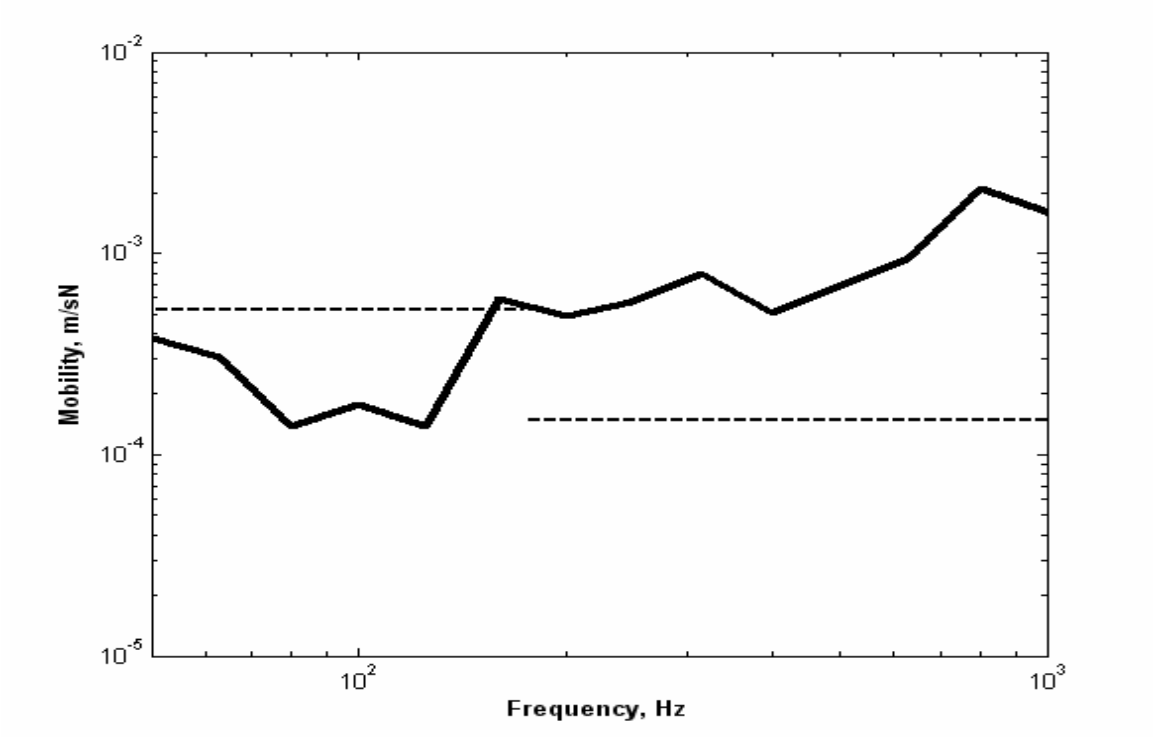

FIGURE 16

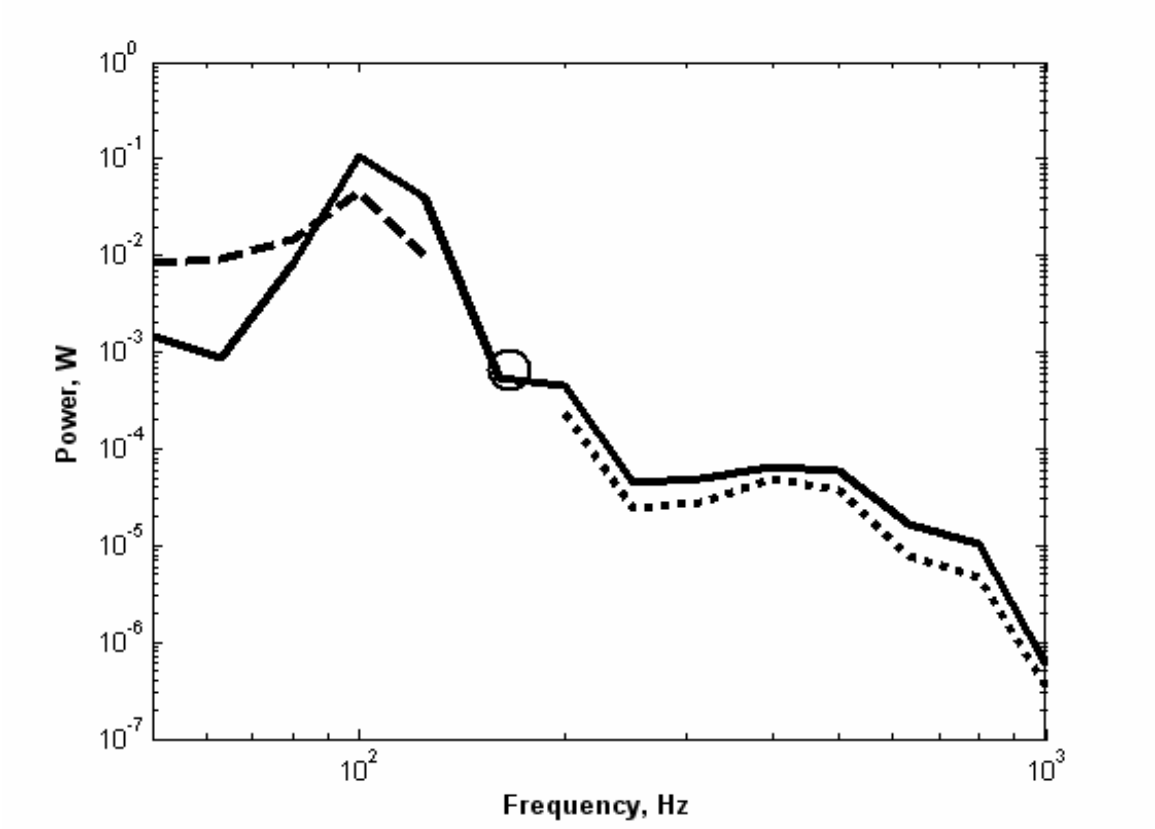

FIGURE 17